Linear and Nonlinear Viscoelasticity of Entangled Multiarm (Pom-Pom) Polymer Liquids

Lynden A. Archer* and Juliani

School of Chemical & Biomolecular Engineering, Cornell University, Ithaca, New York 14853-5201

Received June 9, 2003; Revised Manuscript Received December 1, 2003

ABSTRACT: Stress relaxation dynamics of entangled long-chain branched (LCB) polymers are investigated in small-amplitude oscillatory shear and following nonlinear step shear using model $A_3\mathbf{A}A_3$ multiarm (pom-pom) polymer liquids. A well-characterized multiarm 1,4-polybutadiene melt and its entangled solutions/blends with an unentangled linear 1,4-polybutadiene are the main focus of this study. Relaxation dynamics of multiarm polymers in oscillatory shear are found to be qualitatively similar to predictions of a recent theory for H-shaped polymers based on the tube model. On time scales longer than the relaxation time of the A arms, however, we find that relaxation dynamics of the multiarm polymer backbone **A** are more complex than predicted by this theory. Specifically, the backbone dynamics appear to be dominated by diffusive motion of the branch point in its original (undilated tube). This finding is inconsistent with expectations from theories based on the dynamic dilution ansatz. Stress relaxation dynamics of entangled $A_3\mathbf{A}A_3$ polymers following nonlinear step shear are, paradoxically, simpler. For all polymers studied the nonlinear shear relaxation modulus $G(\gamma,t) \equiv \sigma_{xy}(\gamma,t)/\gamma$ is factorable into separate time-dependent ($G(t)$) and strain-dependent ($h(\gamma)$) functions. In every case, factorability is observed at times beyond a characteristic separability time $t = \lambda_k$ that is comparable to the terminal relaxation time of the polymer. λ_k is also found to manifest a similar dependence on polymer solution concentration as the terminal time. At low shear strains ($\gamma < \gamma_c \approx 5.5$) and for $t \ll \lambda_k$, the shear damping function of all $A_3\mathbf{A}A_3$ liquids is less strain softening than $h(\gamma)$ predicted by the Doi−Edwards theory. For higher shear strains and $t \ll \lambda_k$, multiarm solutions with more than three entanglements per arm manifest a transition to more strain softening, Doi−Edwards-like, damping behavior. The strain γ_c at the transition is a weak function of t and is close to the theoretical estimate for branch point withdrawal in entangled $A_3\mathbf{A}A_3$ molecules. At longer times ($t \geq \lambda_k$), no transition is observed, and the damping function is in fair accord with the Doi−Edwards theoretical prediction for entangled linear polymers over the entire range of shear strains studied. $h(\gamma)$ for multiarm polymer solutions with less than three entanglements per arm do not change slope at the critical strain and are quite similar to the damping function of entangled linear polymer solutions.

1. Introduction

Experimental studies of stress relaxation dynamics of branched polymer liquids have long been recognized as important for understanding structure-processing relationships for commercial long-chain branched (LCB) polyolefins. When such studies are performed using model LCB materials (e.g., branched polymers with precisely known molecular architectures, segmental microstructures, and narrow molecular weight distributions), they can provide insight into more general relationships between molecular architecture, relaxation dynamics, and rheology.This article focuses on the stress relaxation dynamics of model multiarm $A_3\mathbf{A}A_3$ (pom-pom) polymer melts and solutions following imposition of small- and large-amplitude step shear deformations and during small-amplitude oscillatory shear flow.

The H-polymer theory of McLeish et al. provides a good framework for discussing relaxation dynamics of entangled branched polymers. This theory is based on the assumption that stress relaxation in an $A_q\mathbf{A}A_q$ polymer progresses hierarchically and that relaxed sections of a branched molecule dilate the entangled network (tube) in which unrelaxed segments diffuse, in much the same manner as a low molar mass liquid diluent.[1] Molecular segments at the extremities of the A arms are thought to relax first by contour length fluctuations. On longer time scales entire arm sections can relax by arm retraction in a tube that is progressively dilated by previously relaxed arm segments. Once the A arms have completely relaxed, McLeish et al. contend that the polymer backbone or cross-bar, **A**, subsequently relaxes by a combination of contour length fluctuations and reptation diffusion in a tube dilated by the already relaxed arms. This sequence of events is simple enough that it can be captured by a simple analytical theory.[1−3] If correct, this theoretical framework could also be used to predict rheological response of more complex branched structures and perhaps even to extract architectural information from rheological experiments using complex LCB structures.[4]

One consequence of hierarchical relaxation dynamics and dynamic dilution in $A_q\mathbf{A}A_q$ polymers is that these materials should manifest two rubbery plateaus. The first plateau at high frequencies results from the suppression of long-range translational diffusion by entanglements between segments on all parts of the polymer. The second plateau arises from retarded relaxation dynamics of the polymer backbone produced by surviving entanglements between cross-bar segments. If the effective entanglement density of the cross-bar, $s_b = s_{b0}\phi_b^{\alpha}$ is large enough (typically four or larger), the magnitude of the storage modulus in the first plateau G_{N0} should be related to that in the second plateau G_{NII} by a simple formula[3,5]

$$G_{NII} = \phi_b^{\alpha+1} G_{N0} \tag{1}$$

Here $s_{b0} = M_{\mathbf{A}}/M_e(\phi)$ is the number of entanglements

10.1021/ma0347823 CCC: $27.50
Published on Web 01/16/2004

per cross-bar; $\phi_b = M_{\mathbf{A}}/(2qM_A + M_{\mathbf{A}})$ is the volume fraction of cross-bar segments in the polymer; $\alpha = {}^4/_3$ is the dilution exponent for an entangled polymer by a Θ solvent; $M_{\mathbf{A}}$ is the average molecular weight of the cross-bar; M_A is the average arm molecular weight; and $M_e(\phi) = M_{e0}-\phi^{\alpha}$ is the average entanglement molecular weight of a multiarm polymer solution, polymer volume fraction ϕ, and M_{e0} is the entanglement molecular weight in the melt.

If the cross-bar relaxes by simple reptation diffusion in a dilated tube and the friction coefficient of the branch point is assumed to be proportional to the number of arms, the branch point diffusion coefficient is given by

$$D_{bp} = \frac{a^2p^2}{2q\tau_{a0}} \tag{2}$$

and the terminal relaxation time by

$$\tau_{d0} \approx q(1 - x_c)^2 s_b^{\,2} \tau_{a0}^{\,1} \tag{3}$$

Here τ_{a0} is the terminal relaxation time of the arms, a is the cross-bar tube diameter, dilated by relaxed arms, the factor $(1 - x_c)^2$ results from contour length fluctuations, x_c is the cross-bar path length variable at which reptation is preferred over contour length fluctuations for relaxing orientation of the cross-bar,[1] and p is an empirical parameter related to the unknown number, n, of fundamental branch point diffusive steps needed to translate a distance of order one tube diameter ($n \approx p^{-1}$). Ideally, p^2 should be a universal constant of order unity for all entangled polymers. Previous experimental results indicate that its value can vary from ${}^1/_6$ to ${}^1/_{14}$ for $A_q\mathbf{A}A_q$ branched polymer melts[1,3] and by even greater amounts for entangled solutions of branched polymers.[3] Thus, on time scales $t > \tau_{a0}$ the branch point appears to diffuse in a much narrower tube than offered by its relaxed surroundings. This finding can explain another experimental observation, namely that even in materials that satisfy eq 1, eq 3 is not obeyed.[3,5] Specifically, even after arms are relaxed, they exert a surprisingly strong retarding effect on cross-bar relaxation, with the effect that the terminal relaxation time of the cross-bar is a much stronger function of its molecular weight that anticipated for reptation diffusion.[5,7] Fundamental understanding of the cross-bar relaxation process therefore appears to require more detailed knowledge of the tube environment in which entangled cross-bar segments relax.

In a previous study, Archer and Varshney reported that entangled multiarm $A_3\mathbf{A}A_3$ 1,4-polybutadiene melts exhibit a novel transition in the strain dependence of the nonlinear shear relaxation modulus $G(\gamma,t)$ following imposition of step shear.[6] This transition is anticipated theoretically from a simple force balance on an entangled multiarm molecule. At shear strains larger than a critical value γ_c, determined entirely by the number of arms per branch point q, the inward tension on the branch point produced by stretched cross-bar segments is large enough to withdraw relaxed arms into the tube surrounding the cross-bar.[6,7] Arm withdrawal is believed to lead to more strain softening behavior in $G(\gamma,t)$ by providing a mechanism for relaxing cross-bar stretching produced by shear. Thus, when the transition in $G(\gamma,t)$ is observed experimentally, it lends supports to the notion that the branch point of entangled $A_q\mathbf{A}A_q$ branched molecules is constrained to move along the axis of a mean field tube. Despite its obvious uniqueness, the transition in $G(\gamma,t)$ has received little attention in experimental works on branched polymer dynamics. The transition is nonetheless a key feature of tube model-based constitutive theories for branched polymers[8] and therefore deserves more careful investigation.

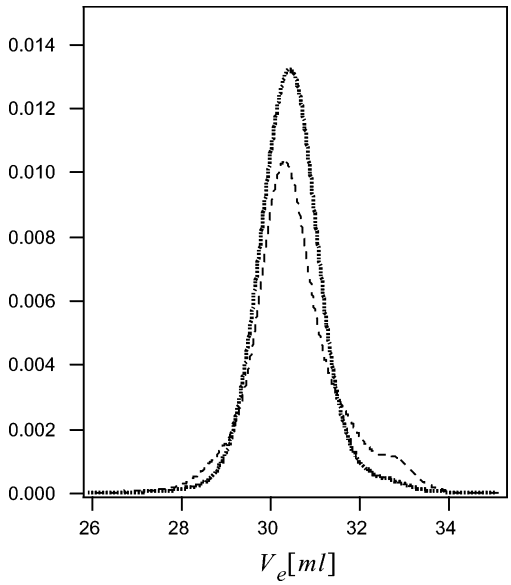

Figure 1. SEC traces of the multiarm $A_3\mathbf{A}A_3$ polybutadiene used in the study before (broken line) and after (dots) fractionation in toluene/methanol mixtures.

2. Experiment

2.1. Materials. The multiarm $A_3\mathbf{A}A_3$ polybutadiene melt used in the present study was synthesized by Polymer Source using a synthesis scheme described in detail elsewhere.[6] Polymer samples suitable for rheological characterization were obtained from repeated fractionation of the synthesized product using toluene/methanol solutions at 30 °C. Size-exclusion chromatographs of the polymer supplied by Polymer Source and the fractionated material used in the study are provided in Figure 1. The molecular weight and polydispersity indices of the unlinked arm ($M_{w,a} = 2.1 \times 10^4$, $M_{w,a}/M_{n,a} = 1.04$) and cross-bar ($M_{w,b} = 8.9 \times 10^4$, $M_{w,b}/M_{n,b} = 1.07$, before terminating with $Si\,Cl_4$) sections of the polymer were determined using size-exclusion chromatography (SEC). The average molecular weight and polydispersity index of the linked $A_3\mathbf{A}A_3$ polymer, $M_{w,ma} = 21.03 \times 10^4$ and $M_w/M_n = 1.17$, were determined using a SEC device equipped with a multiangle laser light scattering detector. It is noteworthy that despite the clearly narrower distribution of the fractionated polymer evident from Figure 1, the polydispersity index reported by SEC is virtually identical to that of the original material.

The $A_3\mathbf{A}A_3$ architecture of the polymer can be confirmed by comparing the overall polymer weight-averaged molecular weight $M_{w,ma} = 21.03 \times 10^4$ measured by light scattering with the total weight-average molecular weight, $M_{w,T} = 6M_{w,a} + M_{w,b} = 21.5 \times 10^4$, estimated for a polymer with an $A_3\mathbf{A}A_3$ architecture. A 2% difference between $M_{w,T}$ and $M_{w,ma}$, though well within the measurement error for molecular weight characterization by multiangle light scattering, could also be caused by a small amount of residual unlinked arms and/or deactivated cross-bar segments present in the material. On the basis of the SEC trace in Figure 1, the latter possibility cannot be ruled out since only about 3.5% of residual cross-bar or just over 2% residual unlinked arms could produce such a difference. It could also explain the larger polydispersity index of the final material in comparison to the polydispersity indices of the unlinked arms and cross-bar. The fact that $M_{w,T} > M_{w,ma}$ is also significant because it indicates that the concentration of higher molecular weight branched species is

Table 1. Characteristic Times for Multiarm Solutions Determined from Experiment

ϕ	ω_c^{-1} (s)	τ_{d0} (s)	λ_k (s)
1.0	508.4	1.3×10^3	480
0.904	214.9	385	253
0.83	124.7	233	162
0.73	20.4	39.9	28
0.64	9.1	13.8	16
0.5	1.0	1.7	2.7
0.34	0.1	0.2	0.4

negligible, which is confirmed by the SEC trace of the fractionated polymer.

H NMR analysis in deuterated benzene indicated that the $A_3\mathbf{A}A_3$ polymer contained approximately 18.6% vinyl (1,2-polybutadiene). Solutions used in the study were created by dissolving the polymer melt in a 1,4-polybutadiene oligomer ($M_w = 1.0 \times 10^3$, $M_w/M_n = 1.11$) with the addition of 0.1% of a commercial hindered phenol antioxidant (Irganox, Ciba). Cyclohexane was used as a cosolvent to facilitate good mixing of polymer and solvent. In previous work, dichloromethane was used for this same purpose.[3] The lower volatility of cyclohexane is advantageous because it eliminates "skin" formation during cosolvent removal. In every case cosolvent was allowed to evaporate at room temperature in a dark chamber for periods ranging from 2 to 4 weeks. Complete removal of the cosolvent was ascertained by gravimetric means.

2.2. Rheological Measurements. Linear and nonlinear viscoelastic properties of multiarm melts and solutions were characterized by small-amplitude oscillatory shear and by large-amplitude step shear measurements using a Paar Physica modular compact (MCR 300) rheometer. All measurements were performed at 23 °C using 8 mm diameter, 1.2° stainless steel cone-and-plate fixtures modified by attaching a single layer of 1 μm silica glass beads to the cone and plate surfaces. As discussed elsewhere,[9,10] this procedure is highly effective for removing measurement errors caused by wall slip. Comparison of storage moduli $G'(\omega)$, loss moduli $G''(\omega)$, and relaxation moduli $G(t)$ data collected at low shear strains using the surface-modified cone-and-plate fixtures with results obtained using 15 mm diameter parallel plates revealed that surface modification lowered the cone angle of the 8 mm fixtures to approximately 1°. Repeat oscillatory shear measurements carried out over a 3 month period using the same polymer and surface-modified cone-and-plate fixtures revealed no change in magnitude and frequency dependence of the storage and loss moduli, confirming the stability of the polymer and bead-treated fixtures.

The rather long relaxation times of the polymers used in the study (Table 1) necessitate long wait periods during sample loading and between successive step shear measurements. For example, a time period of 5 weeks was allowed after loading the melt between rheometer fixtures and the first step strain measurements. During this wait period the normal force exerted by the polymer on the fixtures as well as the polymer response to small-amplitude oscillatory shear were monitored. After about 3 weeks, the latter measurements indicated no change in material properties even though a normal force ranging from 0.5 to 0.7 N was observed. During the remaining 2 week wait period, the normal force decayed below the instrument resolution. A similar procedure was employed for all multiarm polymer solutions used in the study. In the case of the 34% solution, the normal force decayed below the instrument resolution within 4 h after sample loading. To ensure complete relaxation between sequential step shear experiments, multiarm melts and solutions were allowed to relax for periods ranging from 10 times (solution with $\phi = 0.34$) to 30 times (multiarm melt) the terminal relaxation time t_{d0} of the polymer sample. Shear strains were also selected randomly from a fixed set with two repetitions per set to ensure that the relaxation modulus measured at fixed shear strain did not change during the exhaustive measurement periods required to completely characterize a single material.

Storage and loss moduli for the multiarm polymer melt and its solutions are provided in Figure 1a,b. These results were obtained at a fixed temperature of 23 °C, and no attempt was made to extend the frequency range using time−temperature superposition. Even for the limited frequency range covered, the data clearly reveal a linear polymer-like loss minimum at low frequencies and the beginnings of a high-frequency, loss minimum. These features disappear at multiarm solution concentrations where arm entanglements become marginal ($\phi = 0.34$, $M_a/M_e(\phi) \approx 2$) and appear to be a signature of the linear viscoelastic response of $A_q\mathbf{A}A_q$ entangled multiarm polymer liquids. Average relaxation times ω_c^{-1} determined from the crossing of storage and loss moduli and terminal times τ_{d0}, estimated as the reciprocal of the frequency at which $\eta''(\omega)$ manifests a local maximum just prior to the onset of terminal behavior, are provided in Table 1. For multiarm solutions with $\phi > 0.83$, the range of oscillation frequencies possible with the MCR 300 is insufficient to access terminal behavior in $\eta''(\omega)$ at 23 °C. The long-time slope of ln $G(t)$ vs t following small-amplitude step strain was therefore used to estimate terminal relaxation times for these solutions.

3. Results and Discussion

3.1. Linear Viscoelastic Response. Storage, $G'(\omega)$, and loss moduli, $G''(\omega)$, for the multiarm melt are plotted as a function of oscillation frequency in Figure 2a. These results are in excellent accord with $G'(\omega)$ and $G''(\omega)$ obtained by Fourier transformation of the relaxation modulus $G(t)$ determined from small-amplitude step shear measurements. One of the most unsatisfying conclusions of our previous study[3] is that the mechanism by which the branch point of an $A_3\mathbf{A}A_3$ polymer moves following arm (A) relaxation is not known. Specifically, even after accounting for the extra drag produced by the relaxed arms, the branch point seems to execute much smaller jumps than expected if arms are assumed to dilate the tube in which it moves. Figure 3a compares the storage and loss moduli for the multiarm polymer melt with predictions from the H-polymer theory of McLeish et al.[1] under three different branch-point motion scenarios.

(i) The thin dashed line represents the rigorous hierarchical H-polymer theory predictions[1] ($p^2 = 1$, i.e., the branch point diffusivity is analogous to the chain-end diffusivity of a reptating linear molecule, and $s_b = s_b(\phi_b)$; i.e., the mean-field tube in which the branch-point diffuses is uniformly enlarged by relaxed arm segments).

(ii) The dots and corresponding thin continuous line are theoretical predictions for the case where $p^2 = 1$ and the branch point and cross-bar diffuse in an undilated tube ($s_b = s_{b0}$).

(iii) The thick broken and solid lines are the theoretical predictions for the case $s_b = s_b(\phi_b)$, but where the number of branch point hops ($1/p$) needed for the surviving linear chain end to move one tube diameter is kept as an adjustable parameter.

A fourth scenario can occur in which the branch point diffuses in an undilated tube, but the cross-bar diffuses in a dilated tube. The crossover frequency predicted under this scenario is intermediate between (i) and (ii). However, little else about the shape of the predicted storage and loss moduli change. For brevity, we do not pursue this last case any further.

It is clear from Figure 3a that while the rigorous H-polymer theory predictions are in good accord with the experimental data at high frequency, much faster relaxation is predicted (at least by a factor of 10) than observed experimentally. Values of the plateau storage

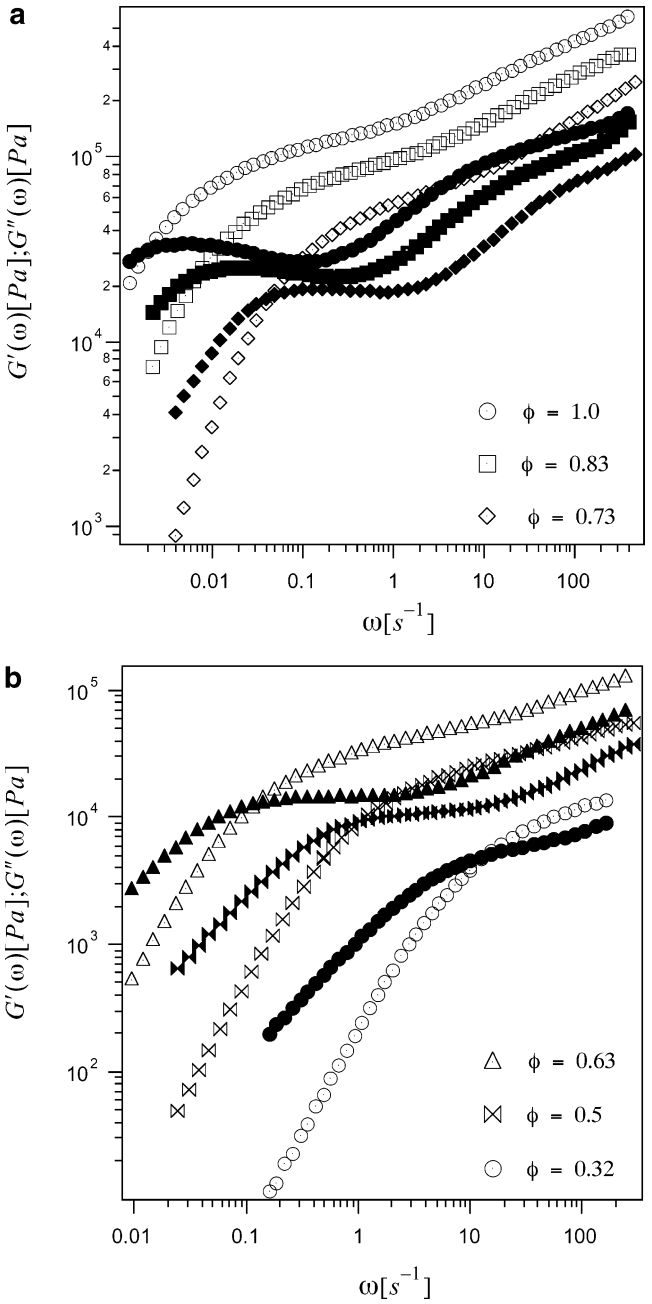

Figure 2. (a) Dynamic storage $G'(\omega)$ (unfilled symbols) and loss moduli $G''(\omega)$ for a 1,4-polybutadiene multiarm $A_3\mathbf{A}A_3$ melt ($M_{w,a} = 2.1 \times 10^4$ and $M_{w,b} = 8.9 \times 10^4$) and its solutions/blends with an unentangled, low-molecular-weight polybutadiene (multiarm polymer volume fraction, ϕ). These measurements were performed at 23 °C using 8 mm diameter cone-and-plate fixtures. (b) Dynamic storage $G'(\omega)$ (unfilled symbols) and loss moduli $G''(\omega)$ for solutions with low multiarm polymer volume fractions ϕ.

modulus $G_{N0} = 1.16$ MPa and entanglement Rouse time $\tau_{e0} = 0.4 \times 10^{-6}$ s used in the comparison are close to results for 1,4-polybutadiene star polymers. The value of τ_{e0} is, however, about 4 times lower than the empirical result obtained from the intersection of the high-frequency Rouse and plateau regimes.[3] With these values of τ_{e0} and G_{N0} an entanglement molecular weight $M_{e0} \approx 2.3 \times 10^3$ is determined to yield the best agreement between theory and experiment. The definition of M_{e0} used in the H-polymer theory in ref 1, and repeated here, is known to yield values of the entanglement molecular weight about 25% larger than determined from the more standard expression $M_{e0} = (4/5)(\rho N_A kT/G_{N0})$.[11] The corrected best-fit entanglement molecular weight is $M_{e0} \approx 1.84 \times 10^3$. This value is close to that obtained from G_{N0}, $M_e = (4/5)(\rho N_A kT/G_{N0}) = 1.6 \times 10^3$ using the plateau modulus and densities reported by Carella et al. for linear polybutadienes with approximately 18% 1,2-isomer content.[12] It is also significantly lower than the value for pure 1,2-polybutadiene ($M_{e0} \approx 3.6 \times 10^3$),[13] which is consistent with the 18% 1,2 isomer content found using H NMR. The best-fit theoretical values determined for the melt ($G_{N0} = 1.2$ MPa, $\tau_{e0} = 0.4 \times 10^{-6}$ s, and $M_{e0} \approx 2.3 \times 10^3$) will be used in all subsequent comparisons between theory and experiment presented in this article.

Now we consider the possibility that the arm constraints prevent the branch point from recognizing the enlarged tube created by relaxed arms. In this case the branch point will diffuse in its primitive, undilated tube, and the cross-bar also reptates in the undilated tube. Storage and loss moduli predicted by the H-polymer theory for this scenario (i.e., for $p^2 = 1$ and $s_b = s_{b0}$) are presented in Figure 3a. Again the predicted high-frequency viscoelastic response is in near quantitative accord with the experimental results. The transition to terminal behavior is predicted to occur at a moderately lower (by a factor of 2) frequency than observed experimentally. Both the storage and loss moduli prior to the transition are also predicted to be larger than the corresponding data from experiment. Enlargement of the effective cross-bar tube diameter by relaxed arms is therefore not entirely to blame for the poor predictions provided by the rigorous H-polymer theory in the terminal regime.

The thick broken and solid lines in the figure are the theoretical predictions for the case $s_b = s_b(\phi_b)$, but where p^2 is considered an adjustable parameter. A value $1/p^2 = 8.5$ yields the correct crossover frequency and good agreement with the experimental storage modulus over the complete frequency range. This value of $1/p^2$ nonetheless produces a more prominent loss maximum prior to the transition to terminal behavior than seen experimentally. Both observations are consistent with previous results for $A_3\mathbf{A}A_3$ polymers[3] and are also in accord with results for $A_2\mathbf{A}A_2$ polymers, where $1/p^2 = 6$ has been reported to provide theoretical predictions of comparable quality.[1,14]

Diffusion of the branch point in a less than completely dilated tube, $p^2 \ll 1$, and a weaker than predicted loss modulus maximum prior to the terminal transition appear to indicate that the long-time dynamics of multiarm $A_q\mathbf{A}A_q$ melts are quite starlike. Figure 3b−d presents comparisons between theory and experiment for multiarm solutions with $\phi = 0.9$, 0.83, and 0.73, respectively. The plateau moduli used for these comparisons are related to the value in the melt by $G_N = G_{N0}\phi^{1+\alpha}$, and the entanglement Rouse time in the solutions is given by $\tau_e = \tau_{e0}\phi^{-2\alpha}$. Here we have utilized the fact that since the microstructure of the multiarm polymer and solvent are similar, the monomeric friction coefficient is not a function of solution concentration. The results in Figure 3b−d consistently show that the only scenario in which the terminal branch point motion can be rigorously claimed to be analogous to that of the chain end of a reptating linear molecule is if $s_b = s_{b0}$; i.e., the terminal relaxation proceeds by diffusion of the branch point in an undilated tube. Indeed for all three solutions the transition to terminal behavior is better

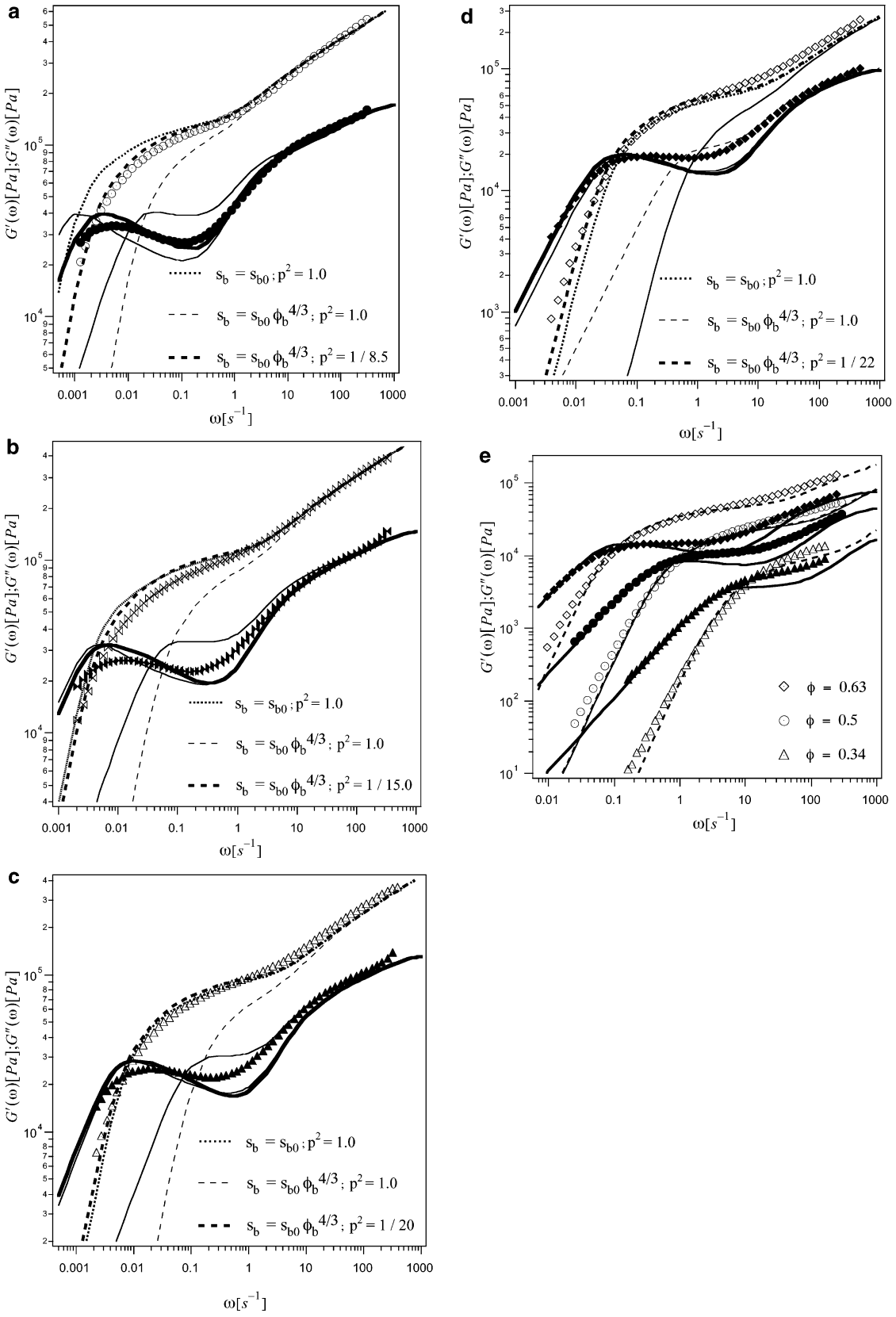

Figure 3. Comparison of experimental data (symbols) and theoretical predictions (lines) of dynamic storage $G'(\omega)$ (broken lines) and loss moduli $G''(\omega)$ (continuous lines) for various multiarm polymer liquids. The three variations of the H-polymer theory used for these comparisons are summarized in the legend and explained in the text. The same model parameters ($G_{N0} = 1.2$ MPa, $\tau_{e0} = 0.4 \times 10^{-6}$ s, and $M_{e0} \approx 2.3 \times 10^3$) are used for all comparisons. (a) Multiarm polymer melt, (b) multiarm polymer solution with $\phi = 0.9$, (c) $\phi = 0.83$, and (d) $\phi = 0.73$. (e) Comparison of experimental data (symbols) and theoretical predictions(lines) of $G'(\omega)$ and $G''(\omega)$ for multiarm solutions with low ϕ. The theoretical predictions are based on the H-polymer theory with $s_b = s_{b0}\phi_b^{4/3}$ and p^2 adjustable. The same model parameters ($G_{N0} = 1.2$ MPa, $\tau_{e0} = 0.4 \times 10^{-6}$ s, and $M_{e0} \approx 2.3 \times 10^3$) are used for all comparisons. p^2 values used for the comparisons and dynamic parameters determined from the theoretical predictions are provided in Table 2.

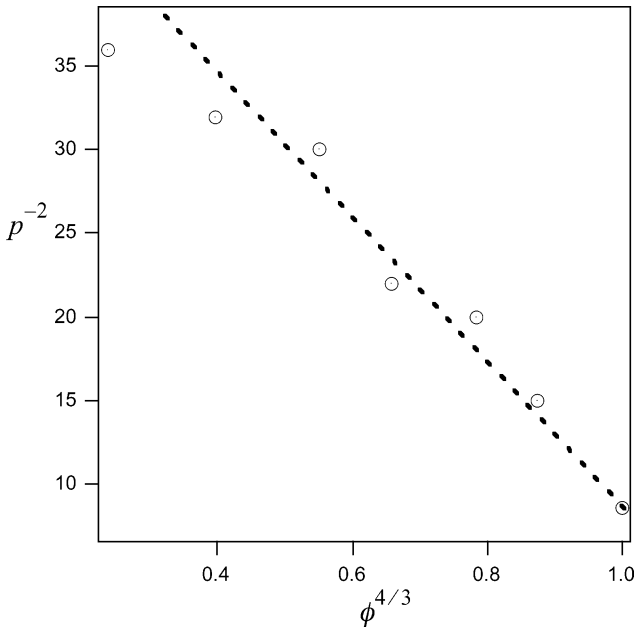

Figure 4. Plot of $1/p^2$ vs dilution variable $\phi^{4/3}$ for all solutions used in the study. In all cases p^2 is the best-fit value required to predict the experimentally determined crossover frequency using the H-polymer theory with $s_b = s_{b0}\phi_b^{4/3}$.

described by this picture than by the alternative case, $s_b = s_b(\phi_b)$ and $p^2 = 1$. It is also noteworthy that a recent analysis of self-diffusion coefficient and zero-shear viscosity data for star polymers arrive at a similar conclusion.[15,16] Namely, that at long times the motion of the branch point of entangled star polymers is in closer agreement with expectations for diffusion in an undilated tube.

Overall the experimental results are best described by the H-polymer theory when p^2 is considered an adjustable parameter. As reported in ref 3, the p^2 value that best reproduces the linear viscoelastic data for multiarm solutions decreases systematically as the concentration of polymer in solution is reduced. Thus, while a value of $1/p^2 = 15$ is required to correctly reproduce the crossover frequency for the multiarm solution with $\phi = 0.9$, a value nearly double this is needed to capture the crossover behavior in a multiarm solution with $\phi = 0.63$. If $1/p^2$ is plotted against $\phi^{4/3}$, as in Figure 4, an inverse relationship is evident over all but the lowest solution concentration. At this concentration the arm entanglement density $M_{w,a}/M_e(\phi)$ is just 2. Physically an inverse relationship between $1/p^2$ and $\phi^{4/3}$ means that the number of diffusive branch point hops needed to translate one tube diameter increases in proportion to the entanglement mesh size (tube diameter) in solution. This result is consistent with our previous observation that the rigorous H-polymer theory ($p^2 = 1$) correctly reproduces the experimental data for the crossover frequency only when the branch point and cross-bar are assumed to diffuse in an undilated tube. Taken together, the two results provide support for the idea that even after the arms of a branched molecule have relaxed, common branch points cannot take advantage of the dilated network to accelerate relaxation.

Polydispersity of the arm and cross-bar sections of the materials used in the study are relatively small; however, previous studies have shown that the relaxation modulus of branched polymers is sensitive to even small amounts of polydispersity, particularly in the arms.[1,14] However, even after the H-polymer theory is corrected for this effect, p^2 values required to fit linear viscoelastic data for H-polymer melts[14] are comparable to the value found here for the $A_3\mathbf{A}A_3$ melt, without the polydispersity correction. Frischknecht et al. also recently reported that significantly smaller p^2 values are required to fit linear viscoelastic data for three-arm asymmetric star polymer melts using a variant of the H-polymer theory with a small polydispersity correction.[14] Significantly, these authors observed that the value of p^2 needed to fit asymmetric star data decreases steadily away from unity as the number of short arm entanglements is reduced. This result is consistent with our observation in Figure 4 that p^2 is an increasing function of the solution volume fraction ϕ and hence arm entanglement density.

All of these results, particularly the small p^2 values needed to reproduce the experimental crossover frequency at low arm entanglement densities, are at odds with expectations based on the dynamic dilution ansatz. The fact that fully relaxed arms do not appear to significantly alter the entanglement environment in which cross-bar segments relax also raises some doubt about the efficiency with which relaxed outer arm sections of a branched molecule can dilate the mean-field tube in which inner sections of the same arm relaxes. Thus, while some dilation might be expected as a consequence of random, local loss of arm constraints, homogeneous tube dilation analogous to that produced by unentangled solvent molecules seems too difficult. Ironically, theoretical predictions based on the dynamic dilution assumption are in best accord with the experimental results at high frequency, where the assumption would appear to be most questionable. Recent work using entangled polyisoprene star polymer melts by Watanabe and co-workers highlight a similar difficulty in describing dynamics of arm sections near a branch point.[17] These authors found that tube models based on dynamic dilution only provide an accurate description of dielectric relaxation of the end-to-end vector of star arms on short and intermediate time scales. Dynamic dilution fails to describe long-time dielectric relaxation dynamics of star arm segments near a common branch point.[17]

While it may be that viscoelastic data for $A_q\mathbf{A}A_q$ polymers with even narrower arm and cross-bar molecular weight distributions than the material used in the present work are needed before definitive statements about the limitations of the dynamic dilution ansatz can be made, the accumulated evidence is that dynamics near the branch point is more complex than envisaged by the H-polymer theory. It is possible that the failure of the theory to predict terminal relaxation dynamics for $A_q\mathbf{A}A_q$ polymers and for asymmetric stars is in some way linked to failure of dynamic dilution observed in stars.[14] However, the fact that p^2 required to fit mechanical data becomes progressively smaller than unity as the number of arm entanglements for the $A_3\mathbf{A}A_3$ solutions and short-arm entanglements for the asymmetric star polymer melts are reduced indicates that other physics are involved. In particular, our observations (a) that p^{-2} decreases nearly in proportion to $\phi^{4/3}$ for multiarm solutions and (b) that a p^2 value of unity provides reasonable predictions under the assumption that the branch point and cross-bar diffuse in an undilated tube strongly indicate that this parameter is not needed in the theory. On the basis of earlier

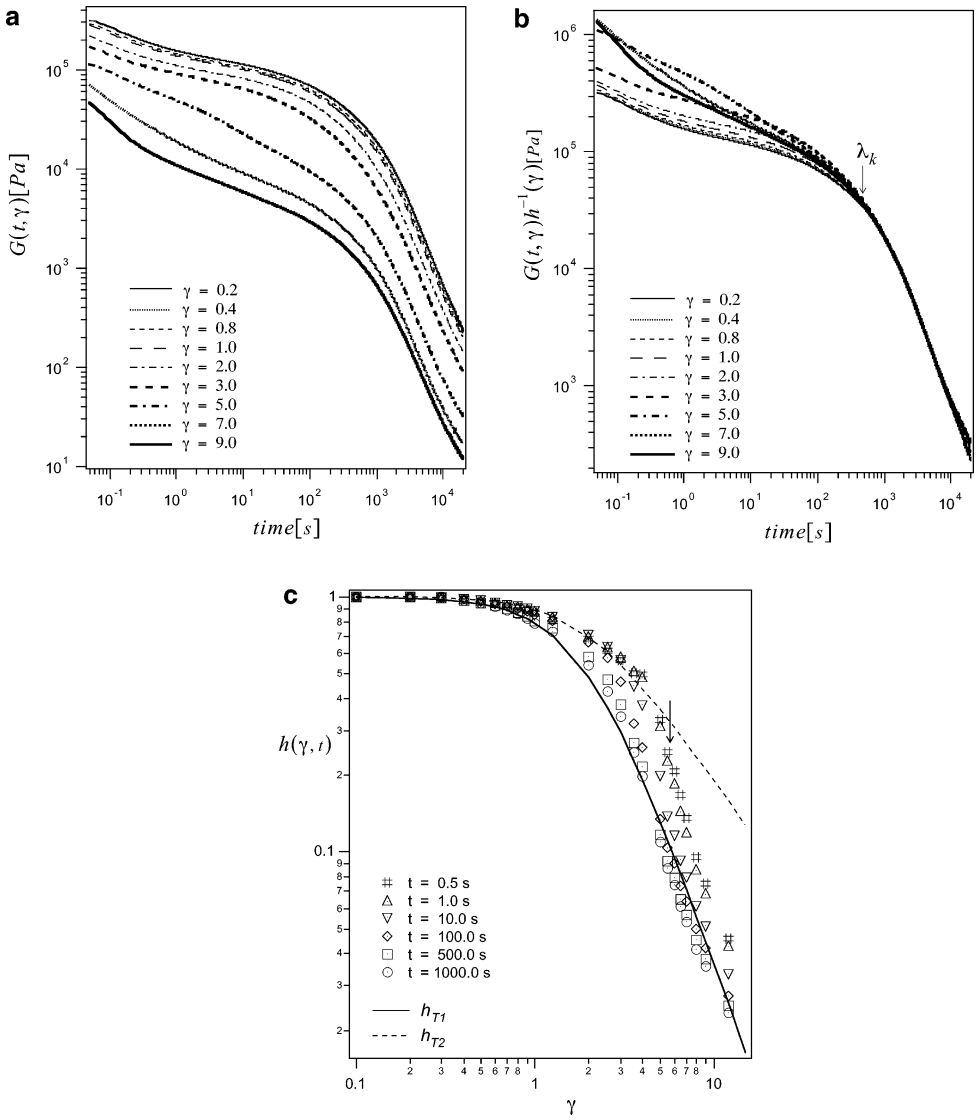

Figure 5. (a) Nonlinear shear relaxation modulus $G(\gamma,t)$ for a 1,4-polybutadiene multiarm $A_3\mathbf{A}A_3$ melt ($M_{w,a} = 2.1 \times 10^4$ and $M_{w,b} = 8.9 \times 10^4$) at 23 °C. Measurements were performed using 8 mm diameter cone-and-plate fixtures roughened by attaching a single layer of 1−3 μm diameter silica spheres. Shear strains γ ranging from 0.2 to 12.0 were used for these measurements. Strain increases from top to bottom in this figure. (b) Shifted nonlinear shear relaxation moduli $G(t,\gamma)h(\gamma)^{-1}$ for the 1,4-polybutadiene multiarm melt at 23 °C. The arrow in the figure identifies the time λ_k beyond which nonlinear shear relaxation moduli $G(\gamma,t)$ can be factorized (approximately) into separate strain-dependent, $h(\gamma)$, and time-dependent, $G(t)$, functions. Values of λ_k for this, and all other materials studied, are tabulated in Table 1. (c) Step shear damping function $h(\gamma,t)$ for the multiarm melt at various times following imposition of step shear. The dashed arrow locates the strain γ_c at which a transition in the shape of $h(\gamma,t)$ is observed, at short times $t \ll \lambda_k$. h_{T1} (dashed line) and h_{T2} (continuous line) are the damping functions predicted by two theories described in the text.

work,[3,5] which show that terminal relaxation does occur in a network dilated by the relaxed arms, there is no doubt that the lost arm constraints do increase the mesh size. However, the branch point and cross-bar appear to be unable to take advantage of the wider mesh spacings to aid their relaxation. We believe that computer simulations for branched polymer dynamics that incorporate nonlocal constraint release effects[18,19] offer the greatest promise for determining the origin of the missing physics in the H-polymer theory.

3.2. Nonlinear Relaxation Dynamics Following Step Shear. Relaxation moduli $G(t,\gamma) \equiv \sigma(t,\gamma)/\gamma$ for the $A_3\mathbf{A}A_3$ multiarm polymer melt are provided in Figure 5a for step strains in the linear and nonlinear viscoelastic regime. Several features of the experimental results are noteworthy. First, at low strains relaxation moduli overlap identically at all times. Second, at large shear strains $G(t,\gamma)$ decreases rapidly with strain, and at long times, plots of log $G(t,\gamma)$ vs log(t) are nearly parallel, irrespective of the shear strain. The first feature of the data is a characteristic of the linear viscoelastic deformation regime. The second feature is more clearly apparent in Figure 5b, where log $G(t,\gamma)$ vs log(t) data at variable shear strain are shifted along the y-axis by an amount $h(\gamma)$ so that data at multiple strains overlap at long times. In this case overlap is most clearly evident beyond a characteristic separability time $\lambda_k \approx 480$ s, which is comparable with the viscoelastic time ω_c^{-1} at which terminal behavior starts (see Table 1) but is just over one-third of the value of the terminal relaxation time τ_{d0} of the polymer. Although weak deviations are apparent at long times, it is quite clear from the data in Figure 5b that the nonlinear relaxation modulus of the multiarm polymer melt is factorable into separate strain- and time-dependent functions. Previous experimental studies have considered the issue of time−strain

factorability in model multiarm polymers,[5,6] but the data in Figure 5b provide the clearest evidence to date supporting time−strain separability in these materials.

Figure 5c reports the damping function $h(\gamma,t)$ of the multiarm melt recorded at various discrete times. Damping function predictions of the Doi−Edwards theory for entangled linear polymers, with the independent alignment assumption (h_{T1})[20] and obtained using the expression $h_{T2}(\gamma) = (1 + (4/15)\gamma^2)^{-1/2}$,[21,22] are included in the figure for comparison. The latter damping form follows from the tube model theory for entangled linear polymers when affinely stretched polymer chains are assumed to only partially recover their equilibrium contour length during Rouse retraction.[21] Here and throughout the article we will use the subscript "T" to indicate a result obtained from theory.

At short times and low shear strain, the measured damping function is less strain softening than h_{T1} and is in better agreement with h_{T2}. Similar short-time damping behavior has been observed previously for entangled linear polymer solutions,[9] as well as for entangled multiarm polymer melts.[6] The unique rheological response of polymers with the $A_3\mathbf{A}A_3$ architecture is evident at higher strains. Specifically, for a shear strain between 5.5 and 6.0 (see arrows), $h(\gamma,t)$ is observed to become more strain softening than apparent at low strains and quickly becomes parallel to the damping function predicted by the Doi−Edwards theory for entangled linear polymers.[20] At progressively longer times, the damping transition is first observed at lower strains and the high-strain damping function approaches the Doi−Edwards prediction. Significantly, for times beyond the factorability time, the damping function of the multiarm melt is quite similar to the Doi−Edwards prediction for almost all shear strains studied. This result is clearly only possible when the cross-bar has completely recovered its equilibrium contour length.

Figure 6a−c summarize the corresponding $G(t,\gamma)$, $G(t,\gamma)h^{-1}(\gamma)$, and $h(\gamma,t)$ plots for the multiarm solution with $\phi = 0.83$. But for the fact that the instantaneous modulus and relaxation time of this material is lower, these results are strikingly similar to those found using the melt. For example, time−strain factorability is observed beyond a time $\lambda_k - 162$ s, which is intermediate between ω_c^{-1} and τ_{d0}. The damping function is also less strain softening than the Doi−Edwards prediction (h_{T1}) at short times and low strains but manifests an unmistakable transition to the more strain-softening damping behavior characteristic of linear polymers at strains above a value around 6. Again, the strain at which the damping transition is first observed is seen to drift slightly downward with time following imposition of the step, and at times beyond the factorability time, the damping function is in rather good accord with the Doi−Edwards prediction for the complete range of shear strains. Similar behavior is observed for multiarm solutions with $\phi = 0.9$, 0.73, and 0.64. $G(t,\gamma)h^{-1}(\gamma)$ and $h(\gamma,t)$ data for the solution with $\phi = 0.73$ are provided in parts a and b of Figure 7. In this case, factorability is observed after a time $\lambda_k \approx 28$ s, and the change of slope of log $h(\gamma)$ vs log(t) at times $t < \lambda_k$ is observed at a shear strain somewhere between 5.5 and 6.0. Again, the damping function at $t > \lambda_k$ is close to the Doi−Edwards prediction for the entire range of shear strains.

$G(t,\gamma)h^{-1}(\gamma)$ and $h(\gamma,t)$ data for a multiarm polymer solution with $\phi = 0.5$ is reported in Figure 8a,b. Using $M_e(\phi) = M_{e0}\phi^{-4/3} = 5.78 \times 10^3$, the average number of entanglements per arm is $M_{w,a}/M_e \approx 3$ and per cross-bar $M_{w,b}/M_e \approx 15$. Time−strain factorability is clearly observed over a broad time range $t > \lambda_k \approx 3$ s. The damping function (Figure 8b) is also very different from those of the more concentrated solutions. Specifically, a smooth transition is observed from damping behavior consistent with h_{T2}, for $t \ll \lambda_k$, to more strain-softening damping behavior for $t \geq \lambda_k$. The shape of the damping function at all times is infact remarkably close to $h(\gamma)$ recently reported for entangled solutions of linear polymers.[9,22] Similar linearlike damping behavior was observed for a multiarm solution with $\phi = 0.34$, $M_{w,a}/M_e \approx 2$. We therefore conclude that the damping function transition observed for multiarm solutions with $\phi \geq 0.6$ is due to the presence of moderately entangled arms. Once these arm entanglements are reduced by dilution, entangled multiarm polymers manifest damping behavior similar to entangled linear polymers.

A transition from elastomer-like damping ($h(\gamma) = 1$) to damping behavior characteristic of entangled linear polymers (h_{T1}) was predicted by the earliest theories for multiarm (pom-pom) polymer dynamics.[7] To our knowledge, this behavior has only been observed experimentally by one group,[6] but even then only for two of the several multiarm melts studied by the authors. The transition in damping behavior is anticipated theoretically for $A_q\mathbf{A}A_q$ multiarm polymers at shear strains where the tension, $F_B = (3kT/a_B)\langle|E\cdot u|\rangle$, on affinely extended cross-bar segments (**A**) just exceeds the outward thermal force on the relaxed arms $F_T = qf_{eq} = 3qkT/a_a$. Here a_B is the diameter of the mean-field tube that restricts lateral motion of cross-bar segments and a_a is the tube diameter for arm segments. $\langle|E\cdot u|\rangle$ is the microscopic tube strain, which can be related to the macroscopic shear strain γ using the relation $\langle|E\cdot u|\rangle \approx (1 + (4/15)\gamma^2)^{0.5}$. Note that, except for the multiarm melt and solution with $\phi = 0.9$, $\tau_{a0,T}$ values estimated from the theory (see Table 2) are generally well outside the time range where the damping transition is observed; the assumption that arms are equilibrated therefore appears to be quite reasonable.

Equating F_B and F_T, it is evident that for shear strains $\gamma > |[(15/4)(\{a_B/a_a\}^2q^2 - 1)]^{1/2}|$ a single cross-bar segment can exert a large enough contraction force to retract down its confining tube, in an analogous manner to a linear entangled molecule. In this case, the damping function is determined only by the strain-induced orientation of cross-bar tube segments and should be similar to the damping function of an entangled linear polymer. Taking $a_B = a_a$ and $q = 3$, the criterion for arm withdrawal is $\gamma > 5.5$. This shear strain is evidently quite close to the strain at which the damping transition is seen experimentally, clearly validating the theoretical prediction. It is nonetheless quite remarkable that a prediction based on simple force balances on individual molecules can result in a macroscopically measurable damping transition. Such correspondence between theoretical expectations and experimental observations is not anticipated in materials with broad distribution of arm and cross-bar molecular weights and with variable number of arms per molecule. We believe that the very fact that the damping transition is seen at shear strains quite close to where they are expected from theory confirms our conclusions about the material's architecture from light scattering and SEC analysis. That the damping transition is observed at nearly identical shear strain for the $A_3\mathbf{A}A_3$ multiarm

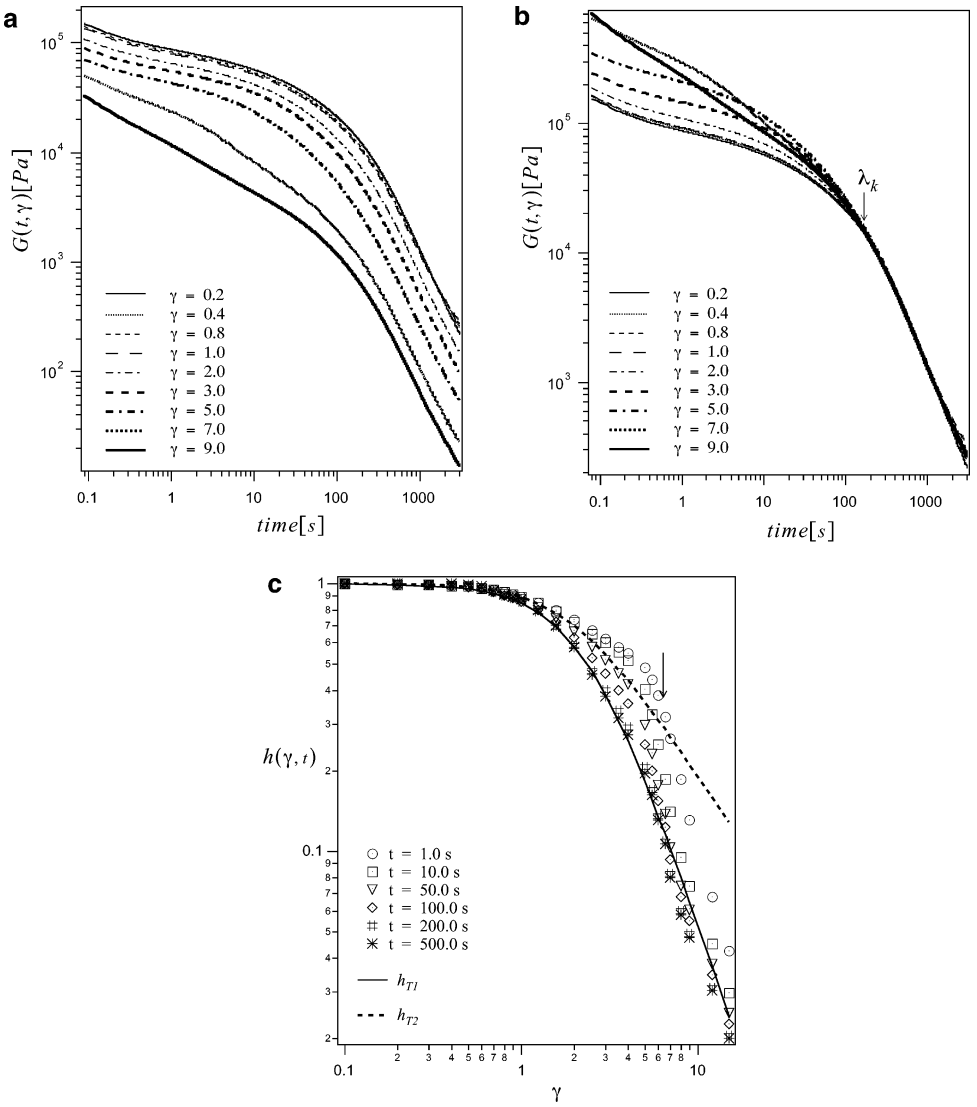

Figure 6. (a) Nonlinear shear relaxation modulus $G(\gamma,t)$ for the multiarm polymer solution with $\phi = 0.83$. These measurements were performed at 23 °C using 8 mm diameter cone-and-plate fixtures roughened by attaching 1−3 μm diameter silica spheres. Shear strains γ ranging from 0.2 to 12.0 were used for these measurements. Strain increases from top to bottom in this figure. (b) Shifted nonlinear shear relaxation moduli $G(t,\gamma)h(\gamma)^{-1}$ for the 1,4-polybutadiene multiarm polymer solution with $\phi = 0.83$. The arrow in the figure identifies the time λ_k (see Table 1) beyond which nonlinear shear relaxation moduli $G(\gamma,t)$ can be factorized (approximately) into separate strain-dependent, $h(\gamma)$, and time-dependent, $G(t)$, functions. (c) Step shear damping function $h(\gamma,t)$ for the multiarm polymer solution with $\phi = 0.83$ at various times following imposition of step shear. The arrow identifies the strain γ_c at which $h(\gamma,t)$ seems to abruptly change shape. h_{T1} (dashed line) and h_{T2} (continuous line) are the damping functions predicted by two theories described in the text.

melt and solutions also rules out most rheological artifacts (e.g., slip at the wall or edge fracture) as the source of this transition. The lack of a transition for solutions with low arm entanglement densities is also consistent with the arm withdrawal mechanism advocated by tube model theories.

On the basis of the uncertainty about branch point motion expressed in section 3.1, the simple result $a_B = a_a$ is surprising. This result follows from a trivial dynamic dilution argument (the entire entanglement structure is dilated homogeneously by relaxed arms), but this argument requires $p^2 = 1$, which is clearly not the case. On the other hand, if one takes $a_B = a_a = a$, where $a = \sqrt{N_{e0}}b$ is the undilated tube diameter, broader if not entirely satisfactory agreement can be obtained between experimental observations and expectations from the tube theory for both the linear and nonlinear viscoelastic response of the multiarm melt and solutions. It is probably possible to learn something about the ratio a_B/a_a and about the evolution of the tube in which the cross-bar diffuses by studying the effect of time on the strain at which the damping transition is observed. Unfortunately, the quality of the current data and the shear strain resolution near the damping transition are insufficient to reach any definitive conclusions. As pointed out earlier, the data in Figures 5c, 6c, and 7b suggest a slight downward drift of the critical strain as time t is varied in the range $t < \lambda_k$. On the basis of the above criterion for arm withdrawal, this would imply that a_B/a_a decreases with time following imposition of step shear, which does not seem plausible. This conclusion also appears to be inconsistent with the fact that the damping function of all materials approach the Doi−Edwards predictions at long times, which would be expected if a_B grows with time (i.e., the terminal dynamics become linearlike, as anticipated from theories based on hierarchical relaxation of multiarm molecules).

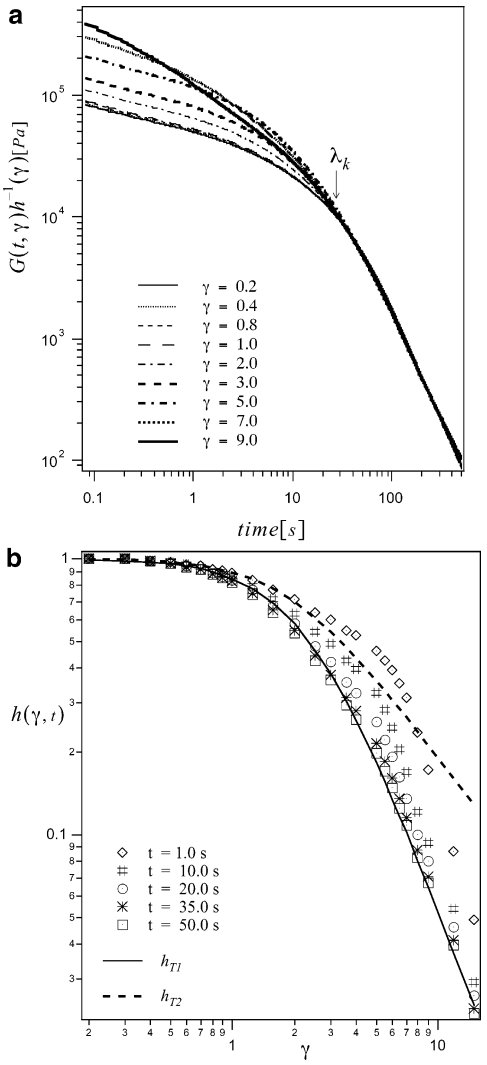

Figure 7. (a) Shifted nonlinear shear relaxation moduli $G(t,\gamma)h(\gamma)^{-1}$ for the 1,4-polybutadiene multiarm polymer solution with $\phi = 0.73$. (b) Step shear damping function $h(\gamma,t)$ for the multiarm polymer solution with $\phi = 0.73$. h_{T1} and h_{T2} are damping functions predicted by two equations described in the text.

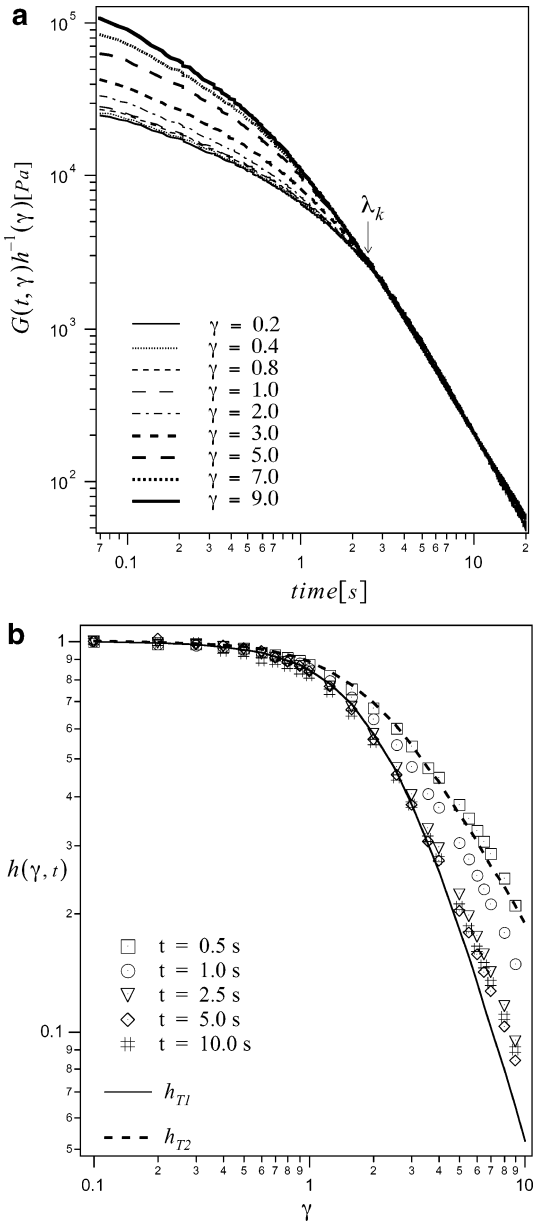

Figure 8. (a) Shifted nonlinear shear relaxation moduli $G(t,\gamma)h(\gamma)^{-1}$ for the 1,4-polybutadiene multiarm polymer solution with $\phi = 0.5$. (b) Step shear damping function $h(\gamma,t)$ for the multiarm polymer solution with $\phi = 0.5$. h_{T1} and h_{T2} are damping functions predicted by two equations described in the text.

We next consider the effect of multiarm solution concentration on the various time scales important to linear and nonlinear rheology of entangled multiarm polymer liquids (see Figure 9). Three of these time scales (ω_c^{-1}, τ_{d0}, and λ_k) were estimated from experimental data and the other two, $\tau_{a0;T} = \tau_{a0}$ and $\tau_{s;T} \approx \lambda_{k;T} = 5\tau_{a0;T}s_b(\phi_b)$, obtained using the H-polymer theory.[1] Figure 9 reveals a particularly simple picture about these time scales. First, it is apparent from the figure that, with the exception of the low concentration $\tau_{a0;T}$ results, all time scales increase exponentially with ϕ. The figure also shows that the theoretical estimate for the separability time $\tau_{s;T}$ is considerably lower than the experimentally determined values of λ_k. λ_k is in fact seen to be closer to the terminal times (ω_c^{-1}, τ_{d0}) for the materials studied here. This last finding is consistent with earlier observations for multiarm polymers[6] as well as for entangled solutions of linear polymers,[9,22] pointing to a possible universal relationship between the terminal relaxation time and the separability time for linearlike molecules. Finally, the fact that the coefficient (slope of Figure 9) is the same for $\tau_{a0;T}$ and all other time scales indicates that the arm retraction time is the fundamental time scale governing slow dynamics of entangled $A_q\mathbf{A}A_q$ multiarm polymers.[1]

Table 2. Characteristic Times and Branch Point Displacement Parameters for Multiarm Solutions Obtained Using H-Polymer Theory[1]

ϕ	ω_{cT}^{-1} (s)	$\tau_{a0,}$T (s)	$\tau_{s;}$T (s)	$1/p^2$
1.0	48.8	0.87	52.1	8.5
0.904	12.2	0.3	15.8	15
0.83	5.9	0.14	6.7	20
0.73	0.8	0.05	2.1	22
0.64	0.2	0.02	0.7	30
0.5		0.006	0.15	32
0.34		0.002	0.03	36

The fact that $A_3\mathbf{A}A_3$ polymers manifest linearlike strain softening properties either at long times or for marginally entangled A arms raises a perhaps obvious question. Namely, what is the damping function of a $A_3\mathbf{A}A_3$ polymer when the number of entanglements per

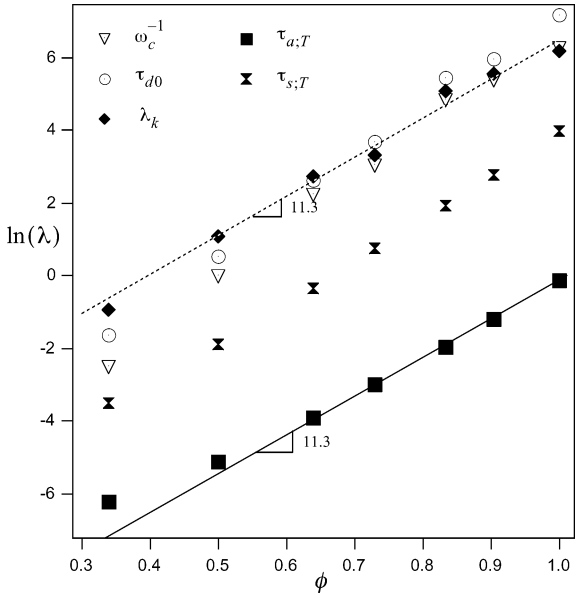

Figure 9. This figure summarizes the effect of multiarm polymer volume fraction ϕ on the various characteristic time scales that govern linear and nonlinear relaxation dynamics of entangled $A_3\mathbf{A}A_3$ multiarm polymer liquids. $\tau_{a;T}$ and $\tau_{s;T}$ are respectively the terminal arm retraction time and the cross-bar stretch relaxation time predicted by the H-polymer theory.

cross-bar **A** is low. An earlier study by Osaki and coworkers using 4-arm star polystyrenes in chlorinated biphenyl reported that the damping function for star polymers, though softer than for linear polymers, is quite close to the result expected from the Doi−Edwards theory with the independent alignment assumption (i.e., $h_{2,T}$).[23,24] Vrentas and Graessley studied stress relaxation dynamics following nonlinear step shear of a four-arm polybutadiene star melt and its solutions in a hydrocarbon oil (Flexon 391) as well as for solutions of a 4-arm star polystyrene in tricrecyl phosphate.[25] For the star polybutadiene melt, the authors report more strain softening than anticipated from the Doi−Edwards theory, while for the polystyrene solution damping behavior less strain softening than the Doi−Edwards prediction was observed. Unfortunately, damping function data reported for the one 4-arm star polybutadiene solution studied are insufficient to reach any concrete conclusion about $h(\gamma)$ for this material.

A limited number of step shear experiments were carried out using entangled solutions of a six-arm, A_6, 1,4-polybutadiene star polymer, $\bar{M}_{w,a} = 7.3 \times 10^4$ and $\bar{M}_w/\bar{M}_n = 1.06$. Solutions were prepared using the same procedures as for the $A_3\mathbf{A}A_3$ materials, and the same low-molecular-weight linear 1,4-polybutadiene was used as solvent. The A_6 star polymer solutions were characterized extensively by oscillatory shear experiments and theory. For brevity, we will not go into details of these results here. These results confirm the architecture and molecular weight of the A_6 1,4-polybutadiene star polymer deduced from gel permeation chromatography and from light scattering measurements.

Figure 10a summarizes $G(t,\gamma)h^{-1}(\gamma)$ for a six-arm star 1,4-polybutadiene solution with polymer volume fraction $\phi = 0.5$, $M_{w,a}/M_e \approx 12$. Time−strain factorability is observed at times $t > \lambda_k \approx 6$ s, which is again comparable to the terminal relaxation time ($\tau_{d0} = 7.9$ s) and crossover time $\omega_c^{-1} = 2.95$ s for the solution. The corresponding damping function is plotted in Figure 10b at various times t following imposition of step strain.

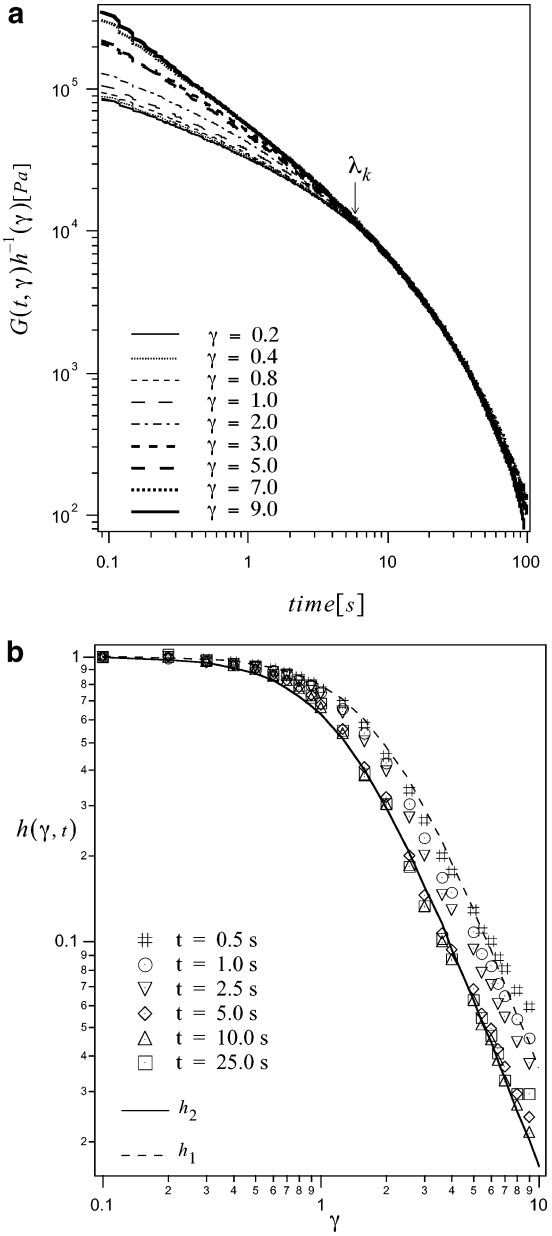

Figure 10. (a) Shifted nonlinear shear relaxation moduli $G(t,\gamma)h(\gamma)^{-1}$ for an entangled solution of a six-arm, A_6, 1,4-polybutadiene (arm molecular weight $\bar{M}_{w,a} = 7.3 \times 10^4$ and $\bar{M}_w/\bar{M}_n = 1.06$) dissolved in a low-molecular-weight linear polybutadiene. These results were obtained at 23 °C using 8 mm diameter cone-and-plate fixtures roughened by attaching 1−3 μm diameter silica spheres and are for a star polymer volume fraction $\phi = 0.5$. (b) Step shear damping function $h(\gamma,t)$ for the star polymer solution with $\phi = 0.5$. h_1 and h_2 are damping functions predicted by two equations described in the text.

Experimental data (symbols) are compared with two analytical forms $h_1(\gamma) = (1 + (4/15)\gamma^2)^{-1}$ and $h_2(\gamma) = (1 + 0.6\ \gamma^2)^{-1}$. It is evident from the figure that at high shear strains the damping function of the star polymer solution decreases with shear strain roughly as $h(\gamma) \sim \gamma^{-2}$. This feature is consistent with observations for linear polymer solutions and for multiarm solutions at times $t > \lambda_k$. It is also consistent with the earlier observations of Osaki et al.[23] Most other features of the damping function for the star polymer solution are unique. For example, the damping form $h_1(\gamma) = (1 + (4/15)\gamma^2)^{-1}$ describes the experimental results very well at early times $\tau < \lambda_k$, indicating that strain softening

behavior qualitatively similar to, but softer than, the Doi−Edwards prediction is observed prior to factorability. This finding is clearly quite different from the short-time ($t \ll \lambda_k$) damping behavior reported in the literature for linear polymer solutions and earlier in the article for entangled multiarm pom-pom polymers; for both classes of materials, an analytical expression of the form ($h(\gamma) = (1 + (4/15)\gamma^2)^{-1/2}$) fairly describes the short-time damping function determined from experiments.

At longer times, $t > \lambda_k$, the damping function for the A_6 1,4-polybutadiene star polymer retains the qualitative form predicted by the Doi−Edwards theory but is more strain softening. Primarily on the basis of these results, we tentatively conclude that the damping function of entangled star polymer solutions is quite different from linear or multiarm $A_3\mathbf{A}A_3$ polymers. Nevertheless, the contradictory results reported in earlier works for the damping function of four-arm star polymers indicate that more experimental data are needed for star polymer systems.

4. Conclusions

We have studied stress relaxation dynamics of a series of entangled $A_3\mathbf{A}A_3$ multiarm 1,4-polymer liquids subject to small-amplitude oscillatory shear and to nonlinear step shear deformations. Our study focuses on a single well-characterized multiarm 1,4-polybutadiene melt and its entangled solutions/blends with an unentangled, low-molar mass 1,4-polybutadiene. Oscillatory shear properties of these materials are found to be in excellent qualitative agreement with a recent tube model theory for H-shaped polymers.[1] This theory is based on the premise that relaxation dynamics of $A_n\mathbf{A}A_n$ branched polymers are hierarchical and that relaxed sections of a multiply branched molecule instantaneously dilate the entanglement network in which unrelaxed sections relax.

Our results indicate that while the high-frequency arm (A) dynamics are reasonably well described by these assumptions, relaxation of the polymer backbone, or cross-bar, **A**, is not. We find that, on time scales much longer than the arm relaxation time, relaxation dynamics of the cross-bar are in closer accord with expectations for diffusive motion of the branch point in its original (undilated tube) than with expectations based on the tube dilation assumption. This finding raises a very interesting general question/paradox about relaxation dynamics of entangled branched polymers. Namely, if relaxed arm segments possessing relaxation times orders of magnitude smaller than the backbone relaxation time do not result in instantaneous dilation of the tube in which cross-bar segments relax, how can exterior segments on the same arm instantaneously dilate the tube environment in which interior ones relax? Yet, the high-frequency oscillatory data, particularly for multiarm solutions with more than six entanglements per arm, are in very good accord with predictions based on dynamic dilution models. We suspect that the answer to this question requires a more complete description of local constraint release dynamics than is captured by current theories for branch polymer relaxation.

Dynamics of entangled $A_3\mathbf{A}A_3$ polymers in nonlinear step shear are even more fascinating. The situation is best described in terms of the nonlinear relaxation modulus $G(\gamma,t) \equiv \sigma_{xy}(\gamma,t)/\gamma$ and the step shear damping function $h(\gamma)$. $G(\gamma,t)$ for all multiarm solutions studied is, for example, factorable into separate strain and time-dependent functions beyond a characteristic separability time $t = \lambda_k$. The separability time is found to be comparable to the terminal relaxation time, irrespective of the number of entanglements per arm. The separability time also varies with polymer volume fraction in solution in the same manner as the terminal time. These findings are remarkably similar to previous observations for entangled solutions of linear polymers. Step shear experiments using entangled six-arm, A_6, 1,4-polybutadiene solutions in low molar mass polybutadienes also reveal time−strain factorability beyond a separability time close to the terminal relaxation time of the polymer. It therefore appears that when rheological artifacts, such as wall slip and edge fracture, are minimized in nonlinear step shear experiments, time−strain factorability is a defining characteristic of entangled solutions of narrow molecular weight distribution polymers irrespective of their architecture.

At short times ($t \ll \lambda_k$) and low shear strains ($\gamma < \gamma_c \approx 5.5$), the shear damping function of all $A_3\mathbf{A}A_3$ multiarm polymer liquids is less strain softening than $h(\gamma)$ predicted by the Doi−Edwards constitutive model. For ($t \ll \lambda_k$) multiarm solutions with more than three entanglements per arm manifest a change to more strain softening, Doi−Edwards like damping behavior (damping functions parallel to, but not necessarily equal to, the Doi−Edwards model prediction) at shear strains $\gamma > \gamma_c$. Significantly, the critical shear strain for the damping transition is found to be nearly insensitive to solution concentration, provided that the arms and cross-bar remain well entangled. The value of γ_c is also quite close to the theoretical estimate for the strain required for the affine tension in the cross-bar to withdraw entangled arms of an $A_3\mathbf{A}A_3$ molecule into the mean-field tube surrounding the cross-bar contour. Both results indicate that the damping transition at $\gamma \approx \gamma_c$ is a characteristic of the $A_3\mathbf{A}A_3$ architecture; its presence provides powerful confirmation of the architectural purity of the materials used in the study.

At longer times the damping transition appears to begin at progressively lower shear strains, until at times $t \geq \lambda_k$ no transition is observed and the damping function agrees with the Doi−Edwards prediction over the entire range of shear strain. This finding is perhaps not unexpected since $\lambda_k \gg \tau_{a0}$, where τ_{a0} is the terminal relaxation time for A arms; any stress that remains at times $t \geq \lambda_k$ therefore originates from orientation of the linearlike cross-bar. This point is confirmed by step shear experiments using $A_3\mathbf{A}A_3$ polymer solutions with low enough concentrations such that the arms are essentially unentangled, but the cross-bar remains entangled. Step shear damping functions for these materials do not change slope at the critical strain and are also remarkably similar (at both short and long times) to damping functions reported for entangled solutions of linear high molar mass polystyrene in diethyl phthalate.

Finally, to investigate the damping function of $A_3\mathbf{A}A_3$ polymers in the opposite situation, namely when the cross-bar is short relative to the arms, a limited number of step shear experiments were performed using entangled solutions of a six-arm star A_6 polybutadiene. Our results indicate that the damping function in these materials is more complicated that those observed in linear or $A_3\mathbf{A}A_3$ polymers with entangled cross-bars. Specifically, we find that while the high-strain asymptotic behavior of the damping function ($h(\gamma) \sim \gamma^{-2}$) is

consistent with the Doi−Edwards model prediction, $h(\gamma)$ for the six-arm star polymer solution is consistently more strain softening than $h(\gamma)$ for the other materials studied. The fundamental origin of this damping behavior is not known.

Acknowledgment. This study was supported by the National Science Foundation Division of Materials Research, Grant DMR0237052. Polymer characterization facilities at Cornell Center for Materials Research, funded through the National Science Foundation Division of Materials Research, were used for characterizing all polymers used in the study.

References and Notes

(1) McLeish, T. C. B.; Allgaier, J.; Bick, D. K.; Bishko, G.; Biswas, P.; Blackwell, R.; Blotteiere, B.; Clarke, N.; Gibbs, B.; Groves, D. J.; Hakiki, A.; Heenan, R. K.; Johnson, J. M.; Kant, R.; Read, D. J.; Young, R. N. *Macromolecules* **1999**, *32*, 6734.
(2) Daniels, D. R.; McLeish, T. C. B.; Crosby, B. J.; Young, R. N.; Fernyhough, C. M. *Macromolecules* **2001**, *34*, 7025.
(3) Juliani; Archer, L. A. *Macromolecules* **2002**, *35*, 6953; *Macromolecules* **2002**, *35*, 10048.
(4) Larson, R. G. *Macromolecules* **2001**, *34*, 4556.
(5) Islam, M. T.; Juliani; Archer, L. A.; Varshney, S. K. *Macromolecules* **2001**, *34*, 6438.
(6) Archer, L. A.; Varshney, S. K. *Macromolecules* **1998**, *31*, 6348.
(7) Bick, D. K.; McLeish, T. C. B. *Phys. Rev. Lett.* **1996**, *76*, 2587.
(8) McLeish, T. C. B.; Larson, R. G. *J. Rheol.* **1998**, *42*, 81.
(9) Sanchez-Reyes, J.; Archer, L. A. *Macromolecules* **2002**, *35*, 5194.
(10) Sanchez-Reyes, J.; Archer, L. A. *Langmuir* **2003**, *19*, 3304.
(11) Larson, R. G.; Sridhar, T.; Leal, L. G.; McKinley, G. H.; Likhtman, A. E.; McLeish, T. C. B. *J. Rheol.* **2003**, *47*, 809.
(12) Carella, J. M.; Graessley, W. W.; Fetters, L. J. *Macromolecules* **1984**, *17*, 2775.
(13) Ferry, J. D. *Viscoelastic Properties of Polymers*, 3rd ed.; Wiley: New York, 1980.
(14) Frischknecht, A. L.; Milner, S. T.; Pryke, A.; Young R. N.; Hawkins, R.; McLeish T. C. B. *Macromolecules* **2002**, *35*, 4801.
(15) Bartels, C. R.; Crist, B.; Fetters, L. J.; Graessley, W. W. *Macromolecules* **1986**, *9*, 785.
(16) Frischknecht, A. L.; Milner, S. T. *Macromolecules* **2000**, *33*, 9764.
(17) Watanabe, H.; Matsumiya, Y.; Inoue, T. *Macromolecules* **2002**, *35*, 2339.
(18) Rubinstein, M.; Colby, R. H. *J. Chem. Phys.* **1988**, *89*, 5291.
(19) McLeish T. C. B. *J. Rheol.* **2003**, *47*, 177.
(20) Doi, M.; Edwards, S. F. *The Theory of Polymer Dynamics*; Oxford University Press: Oxford, 1986.
(21) Mhetar, V. R.; Archer, L. A. *J. Non-Newt. Fluid Mech.* **1999**, *81*, 71.
(22) Archer, L. A.; Sanchez-Reyes, J.; Juliani *Macromolecules* **2002**, *35*, 10216.
(23) Osaki, K.; Takatori, E.; Kurata, M.; Watanabe, H.; Yoshida, H.; Kotaka, T. *Macromolecules* **1990**, *23*, 4392.
(24) Osaki, K. *Rheol. Acta* **1993**, *32*, 429.
(25) Vrentas, C. M.; Graessley, W. W. *J. Rheol.* **1982**, *26*, 359.

MA0347823